LETTERS

Gating pore current in an inherited ion channelopathy

Stanislav Sokolov[1], Todd Scheuer[1] & William A. Catterall[1]

Ion channelopathies are inherited diseases in which alterations in control of ion conductance through the central pore of ion channels impair cell function, leading to periodic paralysis, cardiac arrhythmia, renal failure, epilepsy, migraine and ataxia[1]. Here we show that, in contrast with this well-established paradigm, three mutations in gating-charge-carrying arginine residues in an S4 segment that cause hypokalaemic periodic paralysis[2] induce a hyperpolarization-activated cationic leak through the voltage sensor of the skeletal muscle $Na_V1.4$ channel. This 'gating pore current' is active at the resting membrane potential and closed by depolarizations that activate the voltage sensor. It has similar permeability to Na^+, K^+ and Cs^+, but the organic monovalent cations tetraethylammonium and *N*-methyl-D-glucamine are much less permeant. The inorganic divalent cations Ba^{2+}, Ca^{2+} and Zn^{2+} are not detectably permeant and block the gating pore at millimolar concentrations. Our results reveal gating pore current in naturally occurring disease mutations of an ion channel and show a clear correlation between mutations that cause gating pore current and hypokalaemic periodic paralysis. This gain-of-function gating pore current would contribute in an important way to the dominantly inherited membrane depolarization, action potential failure, flaccid paralysis and cytopathology that are characteristic of hypokalaemic periodic paralysis. A survey of other ion channelopathies reveals numerous examples of mutations that would be expected to cause gating pore current, raising the possibility of a broader impact of gating pore current in ion channelopathies.

Skeletal muscle Na^+ channels generate action potentials in response to nerve stimulation and thereby initiate muscle contraction. They are complexes of pore-forming α and auxiliary β_1 subunits[3–6]. The periodic paralyses are dominantly inherited syndromes that cause episodic failure of skeletal muscle contraction[2]. Hyperkalaemic periodic paralysis and paramyotonia congenita are caused by mutations in the α subunit of skeletal muscle $Na_V1.4$ channels that are widely spread throughout the protein and usually cause a gain of function by impairing fast and/or slow inactivation[7]. Increased Na^+ channel activity leads to depolarization, hyperexcitability, and either repetitive firing or depolarization block. In contrast, hypokalaemic periodic paralysis (HypoPP) is caused by mutations in both the α subunit of the skeletal muscle $Na_V1.4$ channel and the homologous α_1 subunit of the skeletal muscle $Ca_V1.1$ channel, which initiates excitation–contraction coupling[7]. The mutations in both of these large channel proteins target only the outermost two gating-charge-carrying arginine residues in their S4 voltage sensors in domains II and/or IV. The convergence of these mutations on the outermost two gating charges of voltage sensors in two different proteins strongly implicates altered voltage sensor function in this disease. Studies of these mutant Na^+ channels expressed in heterologous cells revealed enhanced fast and/or slow inactivation as the primary common effect[8–11], but it is uncertain how this inhibitory effect causes the dominant inheritance of this disease or its apparent requirement for mutation of gating charges. We therefore explored the hypothesis that unrecognized gain-of-function changes that are unique to the voltage sensor might be caused by these mutations and might contribute to their dominant inheritance.

The voltage sensors of ion channels transduce changes in membrane potential into a conformational change that opens the pore. Gating charges in their S4 transmembrane segments move across the membrane under the influence of the electric field[12,13]. In one mechanistic model, the S4 segments are thought to move outwards through the voltage sensor module by means of a specialized gating pore formed by the segments S1 to S3 (refs 6, 13–18), as presented in detail in a recent high-resolution structural model of the gating process[19]. Consistent with this mechanism is our observation that mutations of the arginine gating charges to smaller, uncharged residues generates gating pore currents resulting from movement of protons and cations through the modified gating pore[20–22]. Mutations of outer gating charges cause gating pore current in the resting state[21,22], whereas mutations of more inward gating charges cause gating pore current in the activated state[22]. Because gating pore current is unique to voltage sensors and is a gain-of-function effect, we tested the HypoPP mutant $Na_V1.4$/R666G for gating pore current.

Wild-type $Na_v1.4$ and R666G channels were transiently expressed in *Xenopus* oocytes together with the Na^+ channel β_1 subunit, and their electrophysiological properties were examined with the cut-open oocyte voltage-clamp technique[23] (Fig. 1). Na^+ currents recorded during depolarizing voltage-clamp steps were generally similar in kinetics and voltage dependence for the wild-type and R666G channels

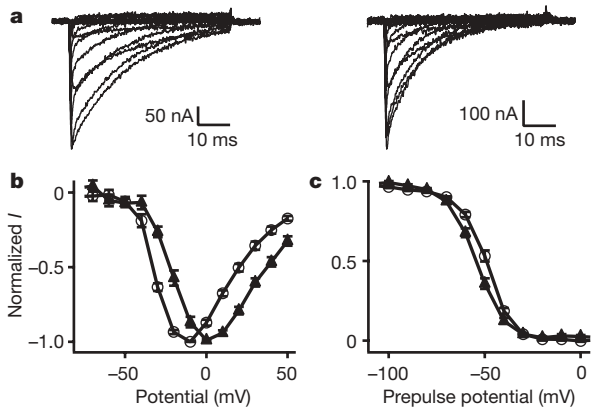

Figure 1 | Central pore Na^+ currents for wild-type $Na_v1.4$ and HypoPP mutant R666G channels. a, Representative Na^+ currents through the central pore of wild type $Na_v1.4$ (left) and R666G (right) channels. **b**, Current–voltage relationships. Mean normalized peak Na^+ current is plotted against test potential for $Na_v1.4$ channels (circles) and R666G (triangles). Voltages for half-maximal activation (V_a) were calculated from conductance-voltage relationships (Supplementary Methods): wild-type $Na_v1.4$, $V_a = -28 \pm 1$ mV, $n = 6$; R666G, $V_a = -15 \pm 3$ mV, $n = 8$. **c**, Voltage dependence of inactivation. The graph shows mean normalized peak Na^+ current during test pulses after 100-ms prepulses to the indicated membrane potentials. Half-inactivation values (V_h) were: wild-type $Na_v1.4$ (circles), $V_h = -49 \pm 1$ mV, $n = 6$; R666G (triangles), $V_h = -55 \pm 1$ mV, $n = 8$ ($P < 0.05$). Error bars denote s.e.m.

[1]Department of Pharmacology, University of Washington, Seattle, Washington 98195-7280, USA.

(Fig. 1a). However, as reported previously[11], there was a trend towards faster inactivation for R666G (Fig. 1a), current–voltage relationships revealed a positive shift in the voltage dependence of activation (Fig. 1b), and the voltage dependence of fast inactivation was shifted to more negative membrane potentials by 6 mV (Fig. 1c).

To detect gating pore currents, we blocked the central pore with 1 μM tetrodotoxin (TTX) and measured leak currents with the normal leak-subtraction protocol turned off. Ionic currents in response to 500-ms voltage steps from a holding potential of −100 mV to test potentials from −140 mV to +50 mV were substantially larger for R666G than for the wild-type channel (Fig. 2a, b). For the wild type, these leak currents were linear (Fig. 2c). In contrast, for R666G a nonlinear component of leak current was observed in the range −50 mV to −140 mV (Fig. 2d). Plotting the mean nonlinear component of ionic current for R666G and the wild type against voltage reveals a highly significant nonlinear inward current in the mutant and none in the wild type (Fig. 2e), similar to gating pore currents (I_{gp}) observed previously for mutations of the outermost gating charges of the $Na_V1.2$ channel IIS4 voltage sensor[22].

The gating pore currents conducted by R666G were much smaller than the central pore Na^+ current. Overexpression of $Na_V1.4$ channels to allow accurate recording of gating pore current usually results in central pore currents that are too large for accurate voltage clamp control in the absence of TTX. However, in favourable cases, we were able to accurately record both gating pore current and central pore current in the same oocyte. A typical example (Fig. 2f) shows that 8 μA of central pore current at −10 mV corresponds to about 80 nA of I_{gp} at −140 mV. As a more physiological comparison, the central pore current at the peak of the action potential (4 μA at +30 mV) is 80-fold greater than the gating pore current at the resting membrane potential (50 nA at −90 mV; Fig. 2f). Although the gating pore current is only about 1.25% of the central pore current, it would be open constantly at the resting membrane potential, whereas the central pore would open for only 1–2 ms during action potentials.

We determined the ion selectivity of the R666G gating pore current for monovalent cations by substituting selected cations for Na^+ in the extracellular solution and measuring the nonlinear component of leak current in the presence of 1 μM TTX to block the central pore (Fig. 3). Surprisingly, even the large organic cation *N*-methyl-D-glucamine ($NMDG^+$) was detectably permeable through this gating pore, as revealed by the nonlinear current increasing towards more negative membrane potentials (Fig. 3a, open squares). For a quantitative comparison of permeability for different monovalent cations, I_{gp} was first measured with 120 mM $NMDG^+$ as the only permeant extracellular monovalent cation. Subsequently, an equal concentration of Na^+, K^+, Cs^+, Li^+ or tetraethylammonium (TEA^+) was added to the recording chamber, and gating pore currents were measured again (Fig. 3a–c). The rank order for the ion selectivity of the gating pore was $Cs^+ \approx K^+ > Na^+ \approx Li^+ \gg TEA^+ \approx NMDG^+$, after correction for the reduced driving force for K^+ resulting from its high internal concentration (Fig. 3c). The R666G gating pore discriminates approximately twofold between Na^+ and K^+ (Fig. 3c), but at the resting membrane potential of a skeletal muscle cell, near the equilibrium potential for K^+ conductance, essentially all gating pore current would be inward movement of Na^+.

Divalent cations block the gating pore (Fig. 3d). Ba^{2+} (6 mM) decreased I_{gp} conducted by Na^+ by 55 ± 9% at −140 mV, which is consistent with a K_d of 4.9 mM, whereas Zn^{2+} (6 mM) completely inhibited gating pore current, indicating a much higher affinity. Complete block by Zn^{2+} strengthens the identification of I_{gp} as a distinct hyperpolarization-activated component of leak current caused by the R666G mutation. Increasing Ca^{2+} concentration from 1.8 mM to 5.9 mM caused a small but significant (27 ± 7%) decrease in I_{gp}, indicating that Ca^{2+} is a weak blocker of I_{gp} (Fig. 3d). Halving the extracellular concentration of Ca^{2+} had no effect on I_{gp}, indicating that Ca^{2+} is not measurably permeant (Fig. 3d). These results suggest that Ca^{2+} leakage through the R666G gating pore is unlikely to contribute to the physiological effects of this mutation.

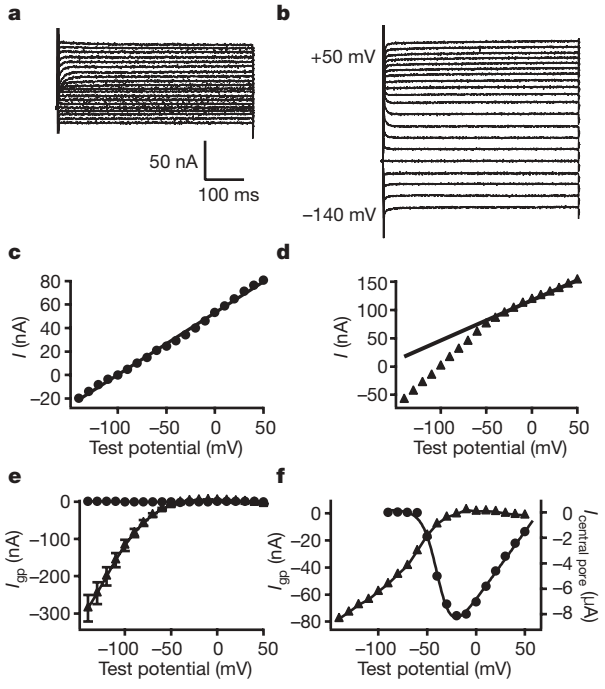

Figure 2 | Gating pore Na^+ currents for HypoPP mutant R666G channels. **a**, **b**, Representative gating pore Na^+ currents in oocytes expressing $Na_v1.4$ (**a**) and R666G (**b**) channels in response to voltage steps ranging from −140 mV to +50 mV without leak subtraction after the blocking of the central pore with 1 μM TTX. **c**, **d**, Relationship of leak current to voltage for $Na_v1.4$ (**c**) or R666G (**d**) channels. **e**, Mean nonlinear component of ionic current for R666G (triangles, $n = 37$) and wild-type (circles, $n = 10$; error bars smaller than symbols) channels. **f**, Comparison of central pore (circles, right axis) and gating pore (triangles, left axis) Na^+ currents in a representative oocyte before and after the addition of 1 μM TTX. Error bars denote s.e.m.

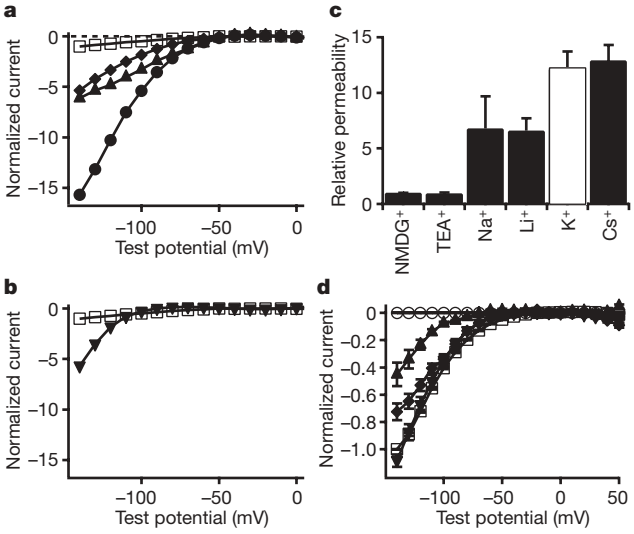

Figure 3 | Ion selectivity of R666G gating pore currents. **a**, **b**, Gating pore currents in representative oocytes were first measured in 120 mM $NMDG^+$ (open squares) and after the addition of Na^+ (triangles), Li^+ (diamonds), or Cs^+ (circles, **a**) or K^+ (inverted triangles, **b**) to the external solution to give a final concentration of 48 mM. Currents are normalized relative to the $NMDG^+$ current at −140 mV in a given oocyte. **c**, Cation selectivity of the gating pore in R666G relative to $NMDG^+$. Data are corrected for ion concentration; those for K^+ (white bar) are corrected for the reduced driving force due to elevated cytosolic K^+ concentration. **d**, Effects of divalent cations on I_{gp}. I_{gp} was recorded with 120 mM Na^+ and 1.8 mM Ca^{2+} in the external solution (squares, $n = 9$) and after the addition of 4.8 mM Ca^{2+} (diamonds, $n = 5$), 6 mM Ba^{2+} (upright triangles, $n = 5$) or 6 mM Zn^{2+} (circles, $n = 4$), or diluting the Ca^{2+} concentration to 0.9 mM (inverted triangles, $n = 4$). Error bars denote s.e.m.

A total of four mutations at only two positions in $Na_V1.4$ channels have been shown to cause HypoPP with complete penetrance: R663H, R666G, R666H and R666S (refs 9, 10, 24). To determine whether gating pore current is a general feature of HypoPP mutations, we tested $Na_V1.4$ channels with the HypoPP mutations R666H and R663H. Both of these mutations conducted a substantial hyperpolarization-activated gating pore current, similar to R666G (Fig. 4). The presence of gating pore current for all three of the HypoPP mutants studied here, including mutations at both relevant positions in the amino acid sequence of $Na_V1.4$ channels, provides strong evidence for an essential role of gating pore current in HypoPP.

Our results show that removal of the positively charged side chain of a gating-charge-carrying arginine residue by the R663H, R666G and R666H mutations creates a gating pore that is measurably permeant to large cations such as $NMDG^+$ and substantially more permeant to the physiological cations Na^+ and K^+. The ion conductance of these gating pores is activated at negative membrane potentials, at which the S4 voltage sensor would be in its most inward position. The effect of these three naturally occurring mutations in $Na_V1.4$ channels therefore resembles those of previous site-directed mutations of the outermost gating charge in $Na_V1.2$ and Shaker K^+ channels[21,22]. Depolarization is likely to move these outermost gating charges towards the extracellular surface of the membrane, out of the narrow point in the gating pore, as a consequence of the conformational change that initiates the activation of these channels[19]. The mutant gating pore would therefore act as a hyperpolarization-activated cation leak in HypoPP skeletal muscle cells. This cation leak would substantially increase resting membrane conductance and Na^+ influx into HypoPP skeletal muscle fibres. These gain-of-function effects would contribute substantially to the dominant inheritance, depolarization, reduced rate of rise and amplitude of the action potential, cytopathology and episodic paralysis correlated with decreased serum K^+ that are the hallmarks of HypoPP[9]. Moreover, a scan of known mutations in other ion channelopathies reveals numerous examples that would be predicted to cause gating pore current (Supplementary Table 1), indicating that gating pore current might contribute significantly to many ion channelopathies. The effects of gating pore current on the pathophysiology of HypoPP and its potential role in other ion channelopathies are considered in more detail in the Supplementary Material.

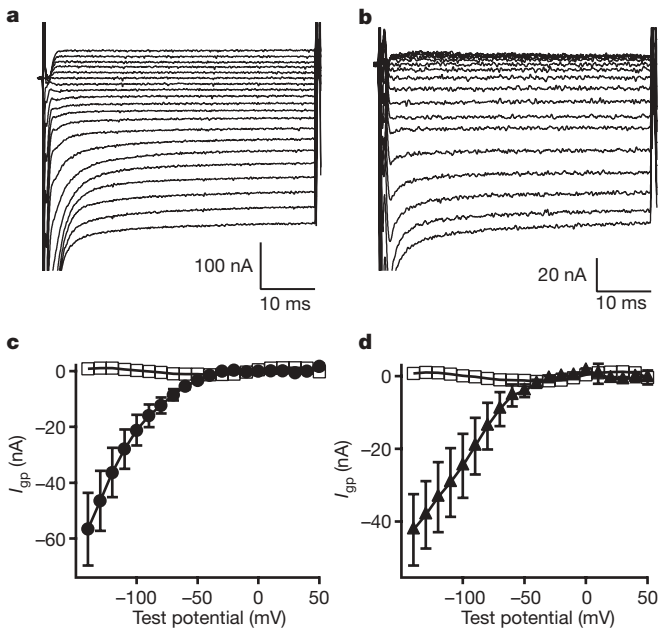

Figure 4 | Gating pore Na^+ current in R663H and R666H HypoPP mutants. **a**, **b**, Representative gating pore Na^+ currents in oocytes expressing R663H (**a**) and R666H (**b**) channels. **c**, **d**, Averaged gating pore currents after linear leak subtraction for R663H (**c**; circles, $n = 8$) and R666H (**d**; triangles, $n = 8$). Results for wild-type $Na_v1.4$ (**c**, **d**; squares, $n = 10$) are reproduced from Fig. 2e. Error bars denote s.e.m.

METHODS

Site-directed mutants in $Na_V1.4$ channels were constructed by polymerase-chain-reaction mutagenesis of a subclone encoding the IIS4 segment and surrounding region of the channel and insertion of the mutant segment into the full-length complementary DNA encoding $Na_V1.4$ as described in Supplementary Methods. RNA encoding wild-type or mutant $Na_V1.4$ plus wild-type β_1 subunits was transcribed *in vitro* and expressed in *Xenopus* oocytes as described in Supplementary Methods. The $Na_V1.4$ channels expressed were analysed with the cut-open oocyte voltage clamp as described[23] (see Supplementary Methods). Gating pore currents were measured in the presence of 1 μM TTX to block the central pore current.

Received 30 November 2006; accepted 15 January 2007.

1. Ashcroft, F. M. From molecule to malady. *Nature* **440,** 440–447 (2006).
2. Venance, S. L. *et al.* The primary periodic paralyses: diagnosis, pathogenesis and treatment. *Brain* **129,** 8–17 (2006).
3. Barchi, R. L. Protein components of the purified sodium channel from rat skeletal sarcolemma. *J. Neurochem.* **36,** 1377–1385 (1983).
4. Trimmer, J. S. *et al.* Primary structure and functional expression of a mammalian skeletal muscle sodium channel. *Neuron* **3,** 33–49 (1989).
5. Isom, L. L. *et al.* Primary structure and functional expression of the beta 1 subunit of the rat brain sodium channel. *Science* **256,** 839–842 (1992).
6. Catterall, W. A. From ionic currents to molecular mechanisms: The structure and function of voltage-gated sodium channels. *Neuron* **26,** 13–25 (2000).
7. Cannon, S. C. Pathomechanisms in channelopathies of skeletal muscle and brain. *Annu. Rev. Neurosci.* **29,** 387–415 (2006).
8. Struyk, A. F., Scoggan, K. A., Bulman, D. E. & Cannon, S. C. The human skeletal muscle Na channel mutation R669H associated with hypokalemic periodic paralysis enhances slow inactivation. *J. Neurosci.* **20,** 8610–8617 (2000).
9. Jurkat-Rott, K. *et al.* Voltage-sensor sodium channel mutations cause hypokalemic periodic paralysis type 2 by enhanced inactivation and reduced current. *Proc. Natl Acad. Sci. USA* **97,** 9549–9554 (2000).
10. Bendahhou, S., Cummins, T. R., Griggs, R. C., Fu, Y. H. & Ptacek, L. J. Sodium channel inactivation defects are associated with acetazolamide-exacerbated hypokalemic periodic paralysis. *Ann. Neurol.* **50,** 417–420 (2001).
11. Kuzmenkin, A. *et al.* Enhanced inactivation and pH sensitivity of sodium channel mutations causing hypokalaemic periodic paralysis type II. *Brain* **125,** 835–843 (2002).
12. Armstrong, C. M. Sodium channels and gating currents. *Physiol. Rev.* **61,** 644–682 (1981).
13. Bezanilla, F. The voltage sensor in voltage-dependent ion channels. *Physiol. Rev.* **80,** 555–592 (2000).
14. Catterall, W. A. Voltage-dependent gating of sodium channels: correlating structure and function. *Trends Neurosci.* **9,** 7–10 (1986).
15. Catterall, W. A. Molecular properties of voltage-sensitive sodium channels. *Annu. Rev. Biochem.* **55,** 953–985 (1986).
16. Guy, H. R. & Seetharamulu, P. Molecular model of the action potential sodium channel. *Proc. Natl Acad. Sci. USA* **508,** 508–512 (1986).
17. Horn, R. Coupled movements in voltage-gated ion channels. *J. Gen. Physiol.* **120,** 449–453 (2002).
18. Gandhi, C. S. & Isacoff, E. Y. Molecular models of voltage sensing. *J. Gen. Physiol.* **120,** 455–463 (2002).
19. Yarov-Yarovoy, V., Baker, D. & Catterall, W. A. Voltage sensor conformations in the open and closed states in ROSETTA structural models of K^+ channels. *Proc. Natl Acad. Sci. USA* **103,** 7292–7297 (2006).
20. Starace, D. M. & Bezanilla, F. A proton pore in a potassium channel voltage sensor reveals a focused electric field. *Nature* **427,** 548–553 (2004).
21. Tombola, F., Pathak, M. M. & Isacoff, E. Y. Voltage-sensing arginines in a potassium channel permeate and occlude cation-selective pores. *Neuron* **45,** 379–388 (2005).
22. Sokolov, S., Scheuer, T. & Catterall, W. A. Ion permeation through a voltage-sensitive gating pore in brain sodium channels having voltage sensor mutations. *Neuron* **47,** 183–189 (2005).
23. Stefani, E. & Bezanilla, F. Cut-open oocyte voltage-clamp technique. *Methods Enzymol.* **293,** 300–318 (1998).
24. Bulman, D. E. *et al.* A novel sodium channel mutation in a family with hypokalemic periodic paralysis. *Neurology* **53,** 1932–1936 (1999).

Supplementary Information is linked to the online version of the paper at www.nature.com/nature.

Acknowledgements We thank E. M. Sharp for technical assistance in molecular biology. This work was funded by research grants from the National Institutes of Health and the Muscular Dystrophy Association to W.A.C.

Author Information Reprints and permissions information is available at www.nature.com/reprints. The authors declare no competing financial interests. Correspondence and requests for materials should be addressed to W.A.C. (wcatt@u.washington.edu).